# Cytoskeletal coherence requires myosin-IIA contractility

**Yunfei Cai[1,*], Olivier Rossier[1], Nils C. Gauthier[1], Nicolas Biais[1], Marc-Antoine Fardin[2], Xian Zhang[1], Lawrence W. Miller[3], Benoit Ladoux[4], Virginia W. Cornish[5] and Michael P. Sheetz[1,‡]**

[1]Department of Biological Sciences, [2]Department of Physics and [5]Department of Chemistry, Columbia University, New York, NY 10027, USA
[3]Department of Chemistry, University of Illinois at Chicago, Chicago, IL 60607, USA
[4]Matiere et Systemes Complexes – Universite Paris 7/CNRS UMR 7057, Batiment Condorcet, 75205 Paris cedex 13, France
*Present address: Department of Developmental and Molecular Biology, Albert Einstein College of Medicine, Bronx, NY 10461, USA
‡Author for correspondence (ms2001@columbia.edu)

*Accepted 18 November 2009*
*Journal of Cell Science 123, 413-423 Published by The Company of Biologists 2010*
*doi:10.1242/jcs.058297*

## Summary

Maintaining a physical connection across cytoplasm is crucial for many biological processes such as matrix force generation, cell motility, cell shape and tissue development. However, in the absence of stress fibers, the coherent structure that transmits force across the cytoplasm is not understood. We find that nonmuscle myosin-II (NMII) contraction of cytoplasmic actin filaments establishes a coherent cytoskeletal network irrespective of the nature of adhesive contacts. When NMII activity is inhibited during cell spreading by Rho kinase inhibition, blebbistatin, caldesmon overexpression or NMIIA RNAi, the symmetric traction forces are lost and cell spreading persists, causing cytoplasm fragmentation by membrane tension that results in 'C' or dendritic shapes. Moreover, local inactivation of NMII by chromophore-assisted laser inactivation causes local loss of coherence. Actin filament polymerization is also required for cytoplasmic coherence, but microtubules and intermediate filaments are dispensable. Loss of cytoplasmic coherence is accompanied by loss of circumferential actin bundles. We suggest that NMIIA creates a coherent actin network through the formation of circumferential actin bundles that mechanically link elements of the peripheral actin cytoskeleton where much of the force is generated during spreading.

**Key words:** Actin, Cell spreading, Coherence, Fibroblast, Myosin-II, Traction force

## Introduction

There have been extensive analyses of the ability of cells to generate forces on matrices or other cells. Many cell types including fibroblasts (Balaban et al., 2001; Cai et al., 2006; Dubin-Thaler et al., 2008; Pelham and Wang, 1999) and smooth muscle cells (Tan et al., 2003) generate traction forces on matrices and the largest forces are found at the cell periphery. Similar force distribution patterns are also observed on epithelial monolayers, where traction forces are supported by cell-cell junctions (du Roure et al., 2005). Cell-based assays demonstrate that force generated by actomyosin-II appears to regulate epithelial cell-cell adhesions (de Rooij et al., 2005; Ivanov et al., 2007; Shewan et al., 2005). In vivo studies are consistent with this. For example, *Drosophila* studies indicate that NMII contraction contributes to the remodeling of epithelial cell junctions and cell intercalations during germ-band elongation (Bertet et al., 2004) and to the apical constriction of ventral cells during gastrulation (Martin et al., 2009). An important element that has not been explicitly defined is the ability of the cell to transmit forces across the cytoplasm (Cai and Sheetz, 2009).

In the case of fibroblasts in vitro, the velocity of cell movement does not generate measurable fluid drag forces. Consequently, traction forces are counterbalanced by opposite traction forces from within the cell. Because large forces are at the cell periphery, and significant counterbalancing forces are not found in the central regions of the cell, forces must be effectively transmitted across the cell cytoplasm through cytoskeletal networks. Of the three cytoskeletal networks, intermediate filaments absorb mechanical stress (Goldman et al., 2008) but their participation in the development of traction force remains inconclusive (Eckes et al., 1998; Holwell et al., 1997). Microtubules are suggested to bear mechanical stress (Brangwynne et al., 2006). Disruption of microtubules enhances formation of stress fibers and cell contraction (Chang et al., 2008). Yet, there has been no evidence to support the direct involvement of microtubules in generation of traction force. Actin stress fibers do generate inward forces on peripheral focal adhesions (Balaban et al., 2001). Remarkably, before the formation of stress fibers, cells appear to generate large forces that are possibly supported by the actin cytoskeleton (Dubin-Thaler et al., 2008; Giannone et al., 2004) in early cell spreading. This can occur by isotropic spreading characterized by three distinct phases: the basal phase (P0), the fast spreading phase (P1), and the slow spreading phase (P2) that is characterized by periodic edge contractions. Another example of large force generation in the absence of stress fibers is the broad lamellipodial region of fish keratocytes that develops high forces (Burton et al., 1999; Galbraith and Sheetz, 1999).

The cellular microfilaments (actin filaments) are suggested to be interlinked into a network (Small and Resch, 2005), presumably by actin-binding proteins such as α-actinin, filamin, NMII etc. Tension change within the actin network induced by ATP causes a change in cell shape (Sims et al., 1992). However, it is still unclear how the actin network transmits matrix forces from one side of the cell to the other. We hypothesize that NMII crosslinks actin filaments (F-actin) into a continuous mechanical network across the cytoplasm (i.e. a coherent network) that is essential for force transmission from one side of the cell to the other side.

Mammalian NMIIs come in three isoforms (IIA, IIB and IIC) that have distinct and overlapping cellular functions (Conti and

Adelstein, 2008; Vicente-Manzanares et al., 2009; Wylie and Chantler, 2008). NMIIA and NMIIB are the primary force generators in fibroblasts (Cai et al., 2006; Lo et al., 2004). Phosphorylation of myosin light chains (MLC), primarily by Rho kinases (ROCK) and MLC kinase (Totsukawa et al., 2004), regulates the NMII activity. ROCK has multiple protein targets including MLC, MLC phosphatase, adducin and moesin (Totsukawa et al., 2004). ROCK activates NMII by phosphorylating MLC and also by inactivating MLC phosphatase to inhibit MLC dephosphorylation (Totsukawa et al., 2004). Specific inhibitors have been developed for studying the functions of NMII, i.e. Y27632 inhibits ROCK and blebbistatin inhibits the ATPase activity of myosin-II. In addition to MLC phosphatase, some other proteins also negatively regulate NMII activity. For example, caldesmon interacts with actin, myosin-II and tropomyosin, and inhibits the ATPase activity of myosin-II (Marston et al., 1998). Caldesmon overexpression causes suppression of traction forces and focal adhesions (Helfman et al., 1999). Thus, there are a variety of ways to inhibit force generation on substrates.

The plasma membrane limits the spreading of cells on substrates, and tension in the plasma membrane inhibits the ability of actin to polymerize at the periphery (Raucher and Sheetz, 2000). Although the tension in the membrane is typically very low (Sheetz, 2001), it can influence the behavior of cells (Keren et al., 2008) and the final shape of cells is heavily influenced by the final membrane area.

We here demonstrate that NMIIA is crucial for the mechanical coherence of cytoplasm. Inhibition of NMII contractility or depletion of NMIIA causes cytoplasm to fragment when cells spread on a matrix.

## Results

### Cell spreading persists when NMII is inactivated, causing loss of cytoplasm continuity and symmetric traction forces

Fibroblasts appear to generate high forces on fibronectin substrates in the contractile phase of cell spreading when periodic edge contractions are observed (Dubin-Thaler et al., 2008; Giannone et al., 2004). In an attempt to study the effect of inhibition of NMII contraction on cell spreading, ROCK was inhibited by Y27632. ROCK inhibition led to a dramatic reduction in the traction force generated by embryonic mouse fibroblasts (supplementary material Fig. S1), in agreement with the literature (Beningo et al., 2006). Interestingly, we observed a striking cell-spreading behavior. The first 2-4 minutes (equivalent to the period of P0 plus P1 phases) of cell spreading was normal. However, spreading persisted longer than usual and often one or more sites in the cell edge broke as most of the cell edge continued to spread. As a result, cells often formed ‘C’ (~45% of cells) or dendritic shapes (~15% of cells, Fig. 1B,C) at early times. The ‘C’ shape formed when breaking occurred at one or two close sites (supplementary material Movie 1) whereas the dendritic shape formed when breaking took place at two or multiple separated sites (supplementary material Movie 2). On careful analysis, it was evident that there was no cytoplasmic network to hold the lamellipodia on the opposite sides of the cell together, i.e. no coherence. When plasma membrane invaded the space normally occupied by the coherent network, it enabled the further spreading of many cells. Thus, the cytoplasm of ‘C’- and dendritic-shaped cells was not able to hold together the adhesive lamellipodia on opposite sides of the cell to form a whole, and we define this phenomenon as ‘loss of cytoplasmic coherence’. Cells regained coherence after washout of Y27632 (supplementary material Movie 3). Y27632-treated cells developed an elongated morphology at later times (1-2 hours after plating), as observed elsewhere (Totsukawa et al., 2004). In contrast to ROCK-inhibited cells, ~97% of control cells were discoidal (Fig. 1A,C) and polarized after 1 hour. Only ~3% of control cells showed either ‘C’ or dendritic shapes (Fig. 1C) that were not severe (supplementary material Fig. S2A,B).

Because ROCK affects other proteins in addition to NMII, we used blebbistatin to determine whether NMII contractility or some other factor affected by Y27632 was important for cytoplasmic coherence. The effect of blebbistatin was very similar to that of Y27632. About 63% of the blebbistatin-treated cells were fragmented, showing ‘C’ (~50%) or dendritic (~13%) shapes (Fig. 1C; supplementary material Fig. S2C). Other cell lines, including NIH3T3 cells (supplementary material Fig. S3; Movie 4) and primary human umbilical vein endothelial cells (data not shown), were also tested and exhibited similar phenotypes upon NMII inhibition. Thus, this phenotype appeared to be quite general. Using fish epidermal keratocytes with different actomyosin structure to mammalian cells (Schaub et al., 2007), previous studies attempting to map the motion and assembly of actin and myosin-II (Schaub et al., 2007) or to examine the directional cytoplasm motility (Verkhovsky et al., 1999) reported keratocyte fragmentation after myosin-II inhibition. We conclude that NMII contraction was important for the formation of a coherent cytoskeletal network in the central region of the cell and that the loss of NMII activity caused the loss of cytoplasmic coherence.

We next asked whether cells pulled on substrates in a coherent manner and whether this required NMII activity. Cells were plated on force-sensing pillars (Cai et al., 2006; du Roure et al., 2005) and the forces of early spreading cells were analyzed. Cells spread on pillars at about half the rate as on glass. Cells generated small traction forces in the P1 phase (Fig. 1D) and large forces in the P2 phase (Fig. 1E) (Dubin-Thaler et al., 2008). The total traction forces in P1 phase were ~10-25% of those in the P2 phase. Importantly, forces were directed inwards, indicating that cells pulled on substrates through a trans-cellular network. In P1 phase, forces applied on pillars were uniformly small (Fig. 1D). However, in P2 phase, large forces were developed at the periphery whereas only small forces were developed in the cell center (Fig. 1E), in agreement with previous studies that analyzed traction forces of cells at well-spread stages (Balaban et al., 2001; Lemmon et al., 2009; Lo et al., 2004; Sunyer et al., 2009; Tan et al., 2003; Undyala et al., 2008). We further analyzed the force distributions and found that the large forces were symmetrically distributed: local large forces on one side counterbalanced local large forces on the other side (Fig. 1E,F), indicating that forces were transmitted across the cytoplasm. When NMII was inhibited, cells exhibited small forces throughout the spreading process and the forces were randomly directed (Fig. 1G,H). Thus, the NMII inhibition decreased both the level and symmetry of traction forces, indicating that correlated traction forces required an active NMII during cell spreading.

### Loss of cytoplasmic coherence is accompanied by disruption of contractile circumferential actin bundles

Because the NMII-inhibited cells lost cytoplasmic coherence in P2 phase, we examined the effects of NMII inhibition on actomyosin organization in early spreading cells. Control cells had circumferential actin bundles in P2 phase (Fig. 2A; supplementary material Movie 5) but not in P0 and P1 phases (supplementary material Movie 5). In late P2, some of the circumferential actin bundles moved inward

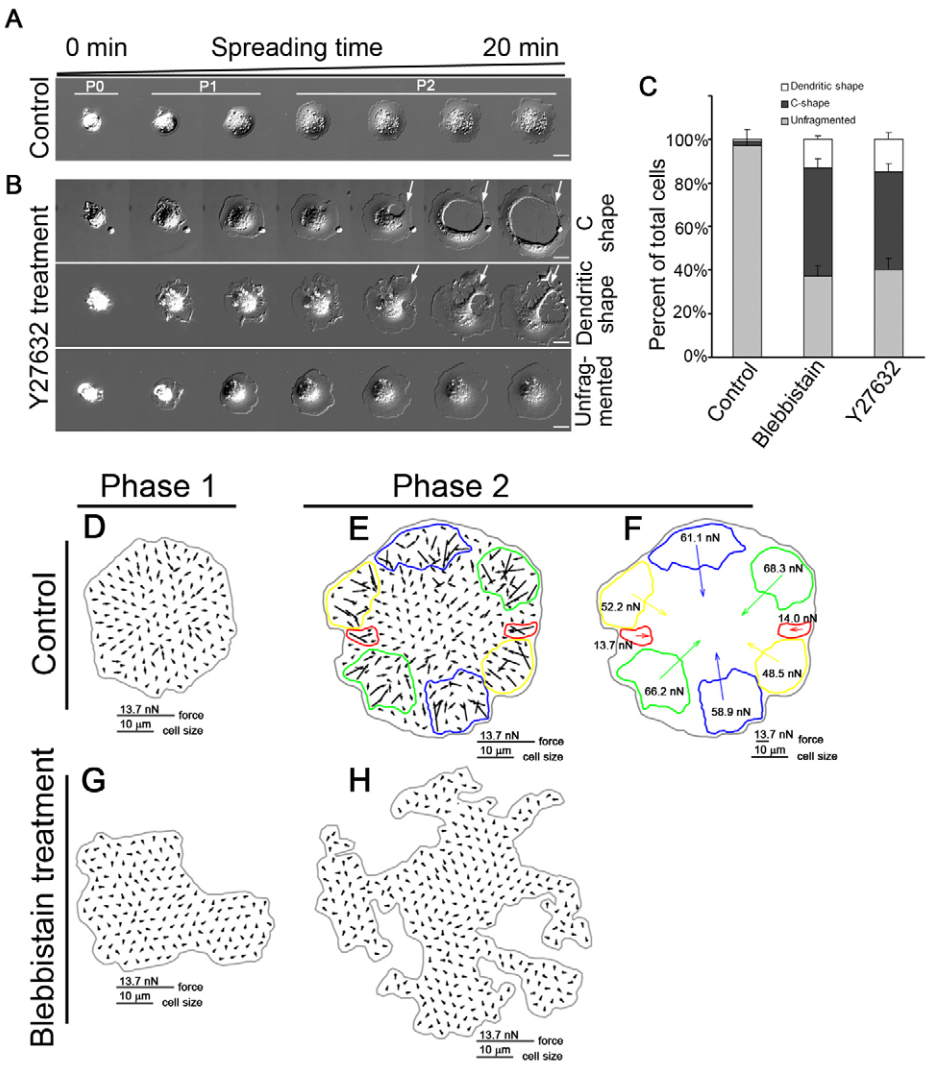


**Fig. 1. Pharmacological inhibition of NMII causes cytoplasm fragmentation.** (**A**,**B**) Selected time-lapse sequential DIC images of control (A) and Y27632-treated (B) cells spreading on fibronectin-coated coverslips at early times. White arrows show cytoplasm rounding and shrinkage. Scar bar: 20 μm. (**C**) Summary of the morphologies of control and inhibitor-treated cells. Of control cells, 2±0.1% are 'C'-shaped, 1±0.1% are dendritic, and 97±7.6% show no fragmentation. Of cells treated with 50 μM blebbistatin, 50±4.1% are 'C'-shaped, 13±1.6% are dendritic, and 37±5.0% show no fragmentation. Of cells treated with 25 μM Y27632, 45±4.0% are 'C'-shaped, 15±3.1% are dendritic, and 40±5.5% show no fragmentation. For each category, >200 cells were sampled from different experiments. Values are mean ± s.d. (**D**,**E**) Maps of inward-pulling forces applied onto fibronectin-coated pillars by control cells in P1 (D) and P2 (E) phases. Cells generate small forces in P1 phase (D) and generate large forces at cell periphery in P2 phase (E). (**F**) Numbers in colors are the net forces (vector sum) of the circled local forces in E. Arrows depict the magnitude and directions of the net forces. An important feature of force distribution is that large forces on one side of cell edge are symmetrically counterbalanced by large forces on the other side of cell edge in P2 phase, as indicated by paired circles with the same colors (E,F). (**G**,**H**) Maps of traction forces applied onto pillars by blebbistatin-treated cells at stages equivalent to P1 (G) and P2 (H) phases. Inhibition of NMII by blebbistatin leads to the generation of very small forces that are randomly orientated.

and contributed to the formation of stress fibers. The ~3% of control cells that displayed 'C' or dendritic shapes also had clear contractile actin bundles and stress fibers (supplementary material Fig. S2B). Inhibition of NMII abolished circumferential actin bundles and stress fibers in both fragmented and unfragmented cells (Fig. 2A). We hypothesized that the contractile circumferential actin bundles endow the cytoplasm with coherence.

Next, we investigated the distributions of NMII isoforms relative to actin structures in early spreading cells. These cells expressed NMIIA and NMIIB but not NMIIC (supplementary material Fig. S4). NMIIA was concentrated on the peripheral nascent actin bundles and the circumferential actin bundles as well as in other regions, including dorsal and ventral stress fibers (Fig. 2A; supplementary material Fig. S5). Little NMIIB was seen on peripheral actin bundles and dorsal stress fibers; instead, the bulk of NMIIB was concentrated on the inner portion of the circumferential actin bundles and ventral stress fibers (Fig. 2A; supplementary material Fig. S5). The differential distributions of NMIIA and NMIIB implied that NMIIA was more likely to be involved in the formation of circumferential actin bundles and stress fibers and therefore in the generation of coherent cytoplasm.

An important question that needed to be addressed was whether significant traction forces were generated during the formation of circumferential actin bundles. We simultaneously examined the GFP-actin dynamics in cells spreading on pillars and the forces generated by the same cells and found that cells did generate large forces in the early P2 phase when there were only circumferential actin bundles and no stress fibers (supplementary material Movie 6; Fig. S6). With the inhibition of NMII, both the large forces and the circumferential actin bundles were lost.

Because NMII inhibition led to continued cell spreading, we examined if and when there was a difference between the spread areas of myosin-inhibited, fragmented and/or unfragmented cells and of control cells during their entire early spreading process (typically, 0-20 minutes). To this end, we followed the spreading history of at least 27 cells in each category (i.e. fragmented cells, unfragmented cells or control cells) using a high resolution assay as previously described (Cai et al., 2006) and plotted the average cell spread area as a function of spreading time (Fig. 2B,C). When comparing the spread areas, we took all the individual spread areas of the unfragmented or fragmented cells and of the control cells at a particular time point and performed the Student's *t*-test analysis. To cover the entire early cell spreading process, the statistical analysis was performed for all the time points. We observed no differences between the early spread areas (the first ~4 minutes) of the unfragmented and fragmented cells and of the control cells.

When analyzing cell spreading in the early P2 phase (during the period of 4-10 minutes), we found that the spread areas of the unfragmented and control cells were similar. However, in late P2, the unfragmented cells spread significantly to a larger area than control cells ($P$<0.05, $n$≥27 cells; Fig. 2B,C), consistent with previous studies (Cramer and Mitchison, 1995; Sandquist et al., 2006; Senju and Miyata, 2009; Wakatsuki et al., 2003). In contrast to the unfragmented cells, the fragmented cells spread to a similar area as control cells during the entire spreading period ($P$<0.08, $n$≥27 cells, Fig. 2B,C). The cytoplasm collapse and rounding in the fragmented cells enabled by the membrane ingression (arrows in Fig. 1B; supplementary material Movies 1 and 2) potentially relieved the membrane tension that might have caused greater exocytosis and spreading in the unfragmented cells at later times. We suggest that there is a greater membrane tension in the unfragmented cells, whereas the fragmentation of cytoplasm would relax that tension. In both cases, we suggest that the loss of cytoplasmic coherence and the restraining force of contraction in the coherent actomyosin network resulted in increased cell spreading.

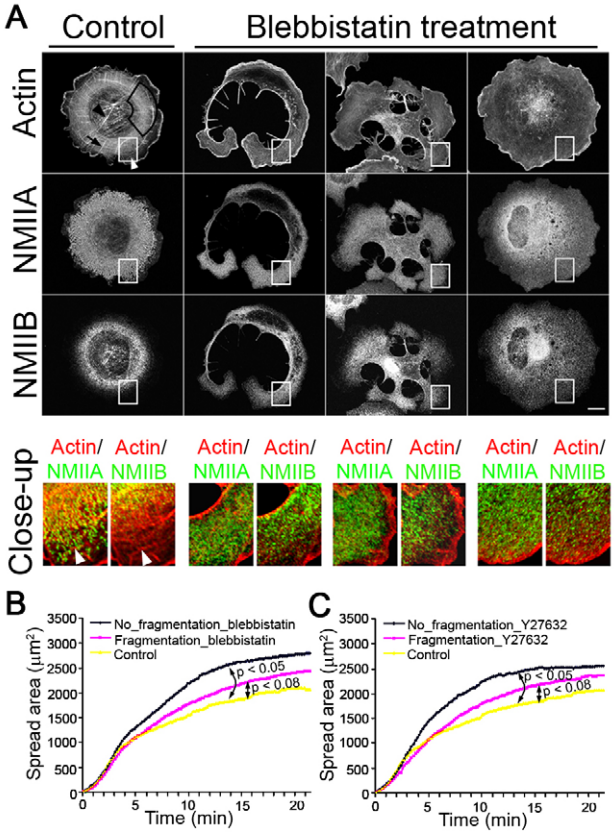


**Fig. 2. NMII-inhibited cells exhibit disorganized actin-NMII structure and unrestrained spreading.** (**A**) Control and blebbistatin-treated cells were plated onto fibronectin-coated coverslips, fixed 20 minutes after plating (in P2), and stained for F-actin NMIIA or NMIIB. White arrowhead, nascent actin arc bundle; black arc-shaped box, circumferential actin bundles; black arrow, dorsal stress fiber; black arrowhead, ventral stress fiber. All single staining images are reconstructed from the entire confocal Z-stacks. Scale bar: 10 μm. Close-up images are overlay of confocal slices. (**B**) Comparison of the spread area between NMII-inhibited cells and control cells (yellow line). Each trace was obtained by plotting the average cell spread area (≥27 cells) as a function of cell-spreading time. The time interval between two sequential time points was 10 seconds. Blebbistatin-treated cells showing no fragmentation (blue line) had a spread area significantly larger than controls ($P$<0.05) 10 minute after initiation of spreading. The spread area within the first 10 minutes of spreading was similar. Cells showing fragmentation (pink line) spread to a similar area as controls ($P$<0.08) during the entire spreading process. The coordinates of a particular point on a given trace (i.e. unfragmented, fragmented or control) are defined by the average cell spread area at a particular spreading time point. When comparing the cell spread area, all the individual spread areas of the unfragmented or fragmented cells and of the control cells at a particular time point were sampled and subjected to Student's $t$-test analysis. The statistical analysis was performed for all the time points. (**C**) The results for Y27632-treated cells were similar to those for blebbistatin-treated cells.

### Caldesmon overexpression and CALI of MLC further reveals the requirement of NMII in maintaining the cytoplasmic coherence

Because caldesmon was able to inhibit the activity of NMII (Helfman et al., 1999), we asked whether it was similarly able to cause continuous cell-edge expansion with the loss of cytoplasmic coherence. At low expression levels, GFP-caldesmon associated with circumferential actin bundles and stress fibers in spreading cells (supplementary material Fig. S7). High levels of GFP-caldesmon expression often abolished circumferential actin bundles and stress fibers (supplementary material Fig. S7), as in trabecular meshwork cells (Grosheva et al., 2006). The assembly of NMIIA was inhibited; however, no clear change in the size of NMIIB clusters was observed in cells expressing high levels of GFP-caldesmon (supplementary material Fig. S7). In the population of cells with high expression of caldesmon, ~50% ($n$=40) had 'C' or dendritic shapes (Fig. 3A; supplementary material Movies 7, 8) mimicking those of inhibitor-treated cells; ~10% of them ($n$=40) appeared to have gaps in the cytoskeleton (supplementary material Fig. S7). These data further supported the idea that NMII contractility was necessary for cytoplasmic coherence.

To examine the requirement of NMII for cytoplasmic coherence, we also conducted local inactivation of NMII by chromophore-assisted laser inactivation (CALI) of MLC. Previous CALI studies have shown that myosins are sensitive to CALI inactivation (Diefenbach et al., 2002; Wang et al., 2003). We expressed a chimeric construct of MLC fused to *E.coli* dihydrofolate reductase (eDHFR) in cells. MLC-eDHFR was labeled with the eDHFR ligand, trimethoprim (TMP) conjugated with fluorescein. TMP has 4000-fold greater affinity for eDHFR than for endogenous mammalian DHFR (Calloway et al., 2007; Miller et al., 2005). After incubation with TMP-fluorescein, cells were spread on a fibronectin substrate. TMP-fluorescein labeling indicated that MLC-eDHFR colocalized with RFP-MLC, indicating that the MLC-eDHFR was functional. Laser bleaching of MLC-eDHFR-TMP-fluorescein generated a small region devoid of fluorescence (Fig. 3C), which rapidly enlarged at early times (Fig. 3D,E; supplementary material Movie 9). This indicated that the continuity of the actomyosin-II network was destroyed by bleaching this region; therefore, tension in neighboring regions was able to pull open the gap in the actomyosin-II network. When the bleached region became larger, fluorescence started to recover, indicating that the contractile actomyosin-II network was being regenerated (Fig. 3D-F). When DIC images were examined, the plasma membrane was not broken. However, the apparent decrease in cytoplasm coherence was seen when cellular features such as actin cables within or close to the irradiated region were examined. The actin cables (e.g. those denoted by green and red lines in Fig. 3G; supplementary material Movie 9) became curved after inactivation of MLC (Fig. 3H-J),

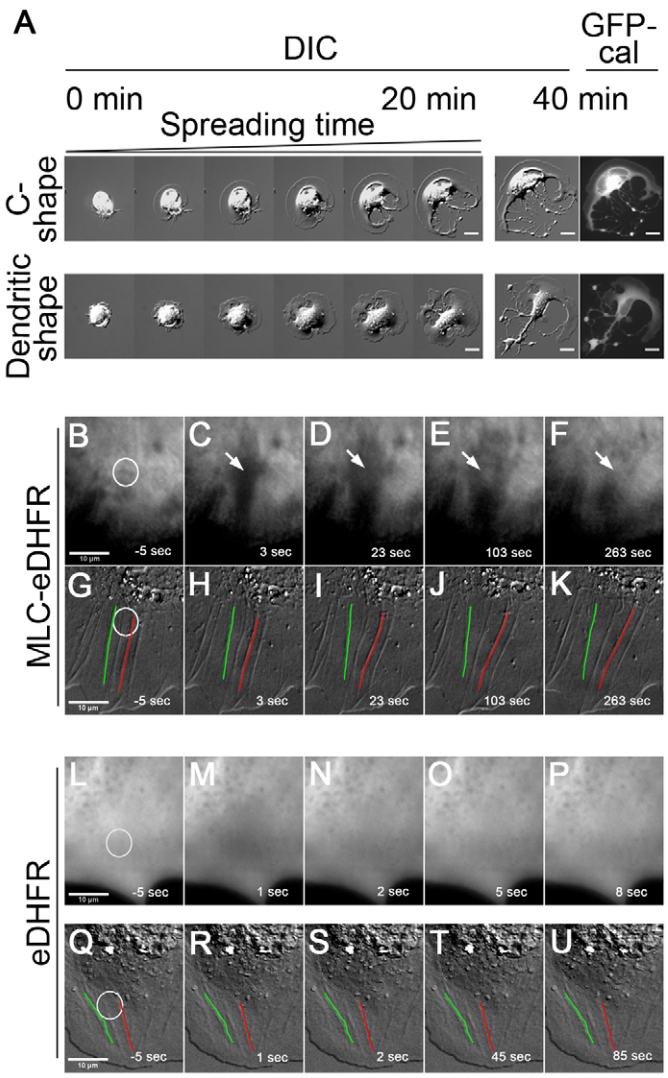


**Fig. 3. Caldesmon overexpression and CALI of MLC reveals requirement of NMII in cytoplasm coherence.** (**A**) Left panels: time-lapse sequential DIC images (within 20 minutes) of spreading cells with a high level of GFP-caldesmon overexpression, showing the dynamic formation of 'C' and dendritic shapes. Right panels: DIC and GFP epifluorescence images of the cells on the left panels at 40 minutes after spreading. Scale bars: 20 µm. (**B-F**) TIRF and (**G-K**) DIC images of the same cell expressing MLC-eDHFR labeled with fluorescein-conjugated TMP before (B,G) and after (C-F, H-K) laser irradiation. Negative times signify time before irradiation. White circles denote the irradiated region. A region devoid of fluorescence forms (arrow in C) after laser irradiation, which is enlarged with time. Meanwhile, fluorescence recovers (arrows in D-F). The decrease of cytoplasmic coherence is clearly displayed by the changes of shapes and positions of actin cables (used as markers) within or close to the irradiated region (G-K) in DIC images. For instance, the upper portion of the actin cable denoted by a green line is curved and clearly moves left, whereas the upper portion of the actin cable denoted by a red line is curved but moves right (H-K). The space between them becomes larger. (**L-P**) TIRF images of a cell. (**Q-U**) DIC images of another cell. Both cells expressed eDHFR that was labeled with fluorescein-conjugated TMP. Images L and Q are pre-irradiation images. Images M-P and R-U are post-irradiation images. eDHFR diffuses in the cell. Following laser irradiation (white circle), the eDHFR fluorescence recovers completely within 5 seconds (M-O). There is no indication of decrease of cytoplasmic coherence because the shapes and positions of marker actin cables (R-U) appear not to change.

indicating that the decrease of coherence in the bleached area allowed contraction in adjacent areas to cause outward curvature of actin cables. Eventually, the actin cables became straight (Fig. 3K), like they were before laser irradiation (Fig. 3G), but with a larger spacing. As a control, cells expressing eDHFR were laser-irradiated after incubation with TMP-fluorescein (Fig. 3L-U). Following laser-irradiation, eDHFR in adjacent regions rapidly diffused into the irradiated region. The eDHFR fluorescence completely recovered within several seconds (Fig. 3M-O; supplementary material Movie 10), making it very difficult to take both fluorescence and DIC images of the same cells. To examine the effect of CALI of eDHFR on cytoplasmic coherence using actin cables as markers, we only took DIC time-lapse images to follow actin cables immediately after laser irradiation. No changes in actin cable position and shape (Fig. 3Q-U; supplementary material Movie 11) were observed. Thus, retraction of the actin cytoskeleton appeared to be a specific effect of photodamage of MLC, because the bleaching of a soluble, fluorescent eDHFR caused no retraction from the bleach site.

### Actin is also required for cytoplasmic coherence, but microtubule and intermediate filament networks are dispensable

The actin cytoskeleton provided a scaffold for many cellular actin-binding proteins including NMII and it was well documented that F-actin depolymerization caused dramatic cell shape changes (Bar-Ziv et al., 1999; Polte et al., 2004; Schliwa, 1982; Zimerman et al., 2004). We applied latrunculin A to cells and observed that >1 µM latrunculin A blocked cell spreading; 600 nM latrunculin A allowed cells to spread slowly but induced large focal F-actin aggregates, as described elsewhere (Schliwa, 1982), and the cytoplasm showed fragmentation as predicted (Fig. 4A), indicating that the actin cytoskeleton was important for cytoplasmic coherence. This is consistent with the notion that actin filaments throughout the cell are interconnected into a network (Small and Resch, 2005).

Because microtubules and intermediate filaments interact with the actin cytoskeleton and have mechanical roles in cell function (Goldman et al., 2008; Ingber, 2003), we examined their roles in cytoplasmic coherence. Depletion of microtubules (10 µM nocodazole) did not induce cytoplasm fragmentation or affect the coherence nature of traction forces (Fig. 4B). The central low force region in the nocodazole-treated cells is smaller than that in the control cells because depolymerization of microtubules, e.g., with nocodazole, enhances cell contractility and formation of stress fibers (Danowski, 1989) via stimulating the activity of RhoA (Chang et al., 2008; Waterman-Storer and Salmon, 1999). As a result of that, cell edge and cell body retract after nocodazole treatment (Ballestrem et al., 2000; Chang et al., 2008), which was also observed in our experiments. The combination of the increased cell contractility and the cell retraction caused the central low force region to become smaller. When we analyzed vimentin knockout (SW-13/c1.2 vim-) cells without detectable vimentin or other cytoplasmic intermediate filaments (Sarria et al., 1990), we found that the cytoplasmic coherence and the force coherence appeared normal (Fig. 4B).

### F-actin assembly, not the cell-substrate adhesion, determines fragmentation sites in the absence of NMII activity

Because NMII-inhibited cells that were spreading on fibronectin had no contractile actin bundles and focal adhesions, we asked which

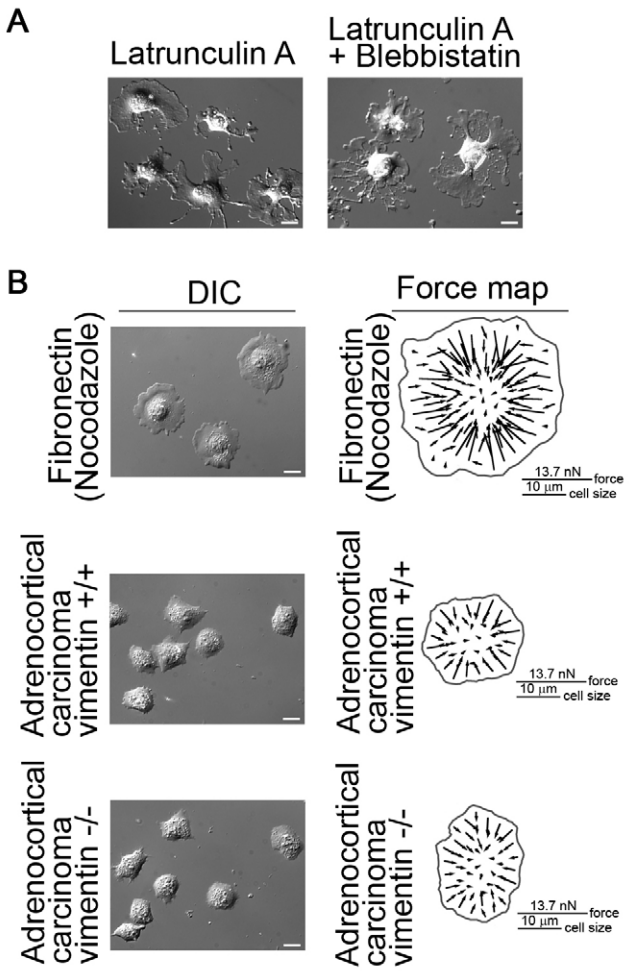


**Fig. 4. Microtubules and intermediate filaments are not essential for cytoplasmic coherence whereas actin cytoskeleton is needed.**
(**A**) Depolymerization of F-actin alone or in combination with NMII inhibition induces cytoplasm fragmentation of fibroblasts on fibronectin substrate. (**B**) Fibroblasts treated with 1 μM nocodazole retain cytoplasmic coherence on fibronectin substrate and have the same force distribution patterns as control cells shown in Fig. 1, generating inward-pulling large forces at cell periphery and small forces in cell center. Human adrenocortical carcinoma cells (vimentin$^{+/+}$) and human adrenocortical carcinoma vimentin knockout cells (vimentin$^{-/-}$) also exhibit coherent cytoplasm and generate forces with similar patterns as control fibroblasts. Scale bars: 20 μm.

of these was the major factor responsible for cytoplasm fragmentation in NMII-inhibited cells. To address this, we examined cells spreading on poly-lysine. In spite of the enhanced cell-substrate adhesion on poly-lysine, the NMII-inhibited cells exhibited fragmentation (Fig. 5A). They had no focal adhesions, as indicated by the diffuse paxillin staining (Fig. 5B). We conclude that it was the lack of NMII contractility and the subsequent lack of actin bundling that caused cytoplasm fragmentation, not the loss of focal adhesions. This idea was also supported by a recent study (Zhang et al., 2008) showing that talin-depleted cells retained NMII contraction but did not have focal adhesions. These cells initially spread and then quickly rounded up as a result of NMII contraction. Expression of talin head domain enabled talin-depleted cells to stay in a well-spread state for a long period without inducing formation of focal adhesions. In both cases, there was no cytoplasm fragmentation.

To search for the determinants of the initial fragmentation sites and for why a fraction of cells did not fragment in the face of NMII inhibition, we compared the Arp2/3 and F-actin staining between NMII-inhibited cells spread on fibronectin and on poly-lysine substrates (Fig. 5B). In cells spread on both substrates, Arp2/3 was rarely present along the edge of fragmented sites but clearly accumulated along the cell edge in unfragmented regions; F-actin was wavy and much less was seen at the fragmented regions compared to unfragmented regions. Often, a narrow F-actin band along the edge of fragmented regions was seen, particularly at advanced stages of development of 'C' and dendritic shapes. This was probably caused by the condensation of F-actin during cytoplasm collapse because there was little actin polymerization, as indicated by the lack of Arp2/3 staining. Together, these data indicated that when NMII was inhibited, a relative lack of actin polymerization was the cause of fragmentation, which was further supported by the decrease in GFP-actin intensity before the initiation of fragmentation (Fig. 5C).

### Effects of depletion of NMII on cytoplasmic coherence

Because NMII isoforms have been shown to have overlapping functions, we used isoform-specific siRNAs to investigate whether this was the case for cytoplasmic coherence (supplementary material Fig. S4). Control and NMII-depleted cells were spread on fibronectin for 20-30 minutes and immunofluorescence staining was used to identify NMII-depleted cells. NMIIA depletion (Fig. 6A) resulted in a decrease in circumferential bundles, stress fibers and focal adhesions, consistent with previous reports (Even-Ram et al., 2007; Sandquist et al., 2006). The extent of decrease was dependent on the level of NMIIA depletion. Cells with >95% depletion of NMIIA (based on the intensity of total fluorescence in over 90 cells from different independent experiments) had almost no circumferential bundles and stress fibers. About 32% of these cells showed loss of cytoplasmic coherence: ~14% displayed a 'C' shape (middle panel in Fig. 6A) or dendritic shape and ~18% had gaps in actin network in the central region of cytoplasm (bottom panel in Fig. 6A), reminiscent of the macro-apertures in RhoA-knockdown and ROCK-inhibited endothelial cells (Boyer et al., 2006). Although the remaining 68% cells did not present 'C' shapes, dendritic shapes or gaps, their cytoplasm appeared very thin. In contrast to NMIIA depletion, NMIIB depletion (Fig. 6B) caused no changes in circumferential actin bundles, stress fibers and focal adhesions from control cells, suggesting that NMIIB was not required for cytoplasmic coherence. These observations indicated that NMIIA-induced contractility was essential for cytoplasmic coherence.

## Discussion

Our findings show that NMIIA contractility is required for maintaining a coherent actin cytoskeleton that prevents spreading cells from fragmenting as a result of continued spreading. This coherent NMIIA-actin cytoskeleton constitutes a continuous mechanical link from one side of the cell to the other that is needed to develop matrix traction forces and to resist the spreading forces generated presumably through actin assembly (Footer et al., 2007; Pollard and Borisy, 2003; Prass et al., 2006). The large matrix forces in early spreading cells are symmetric, indicating that spreading cells have a network that transmits force directly across cytoplasm. When NMII activity is inhibited throughout the cells, they fragment

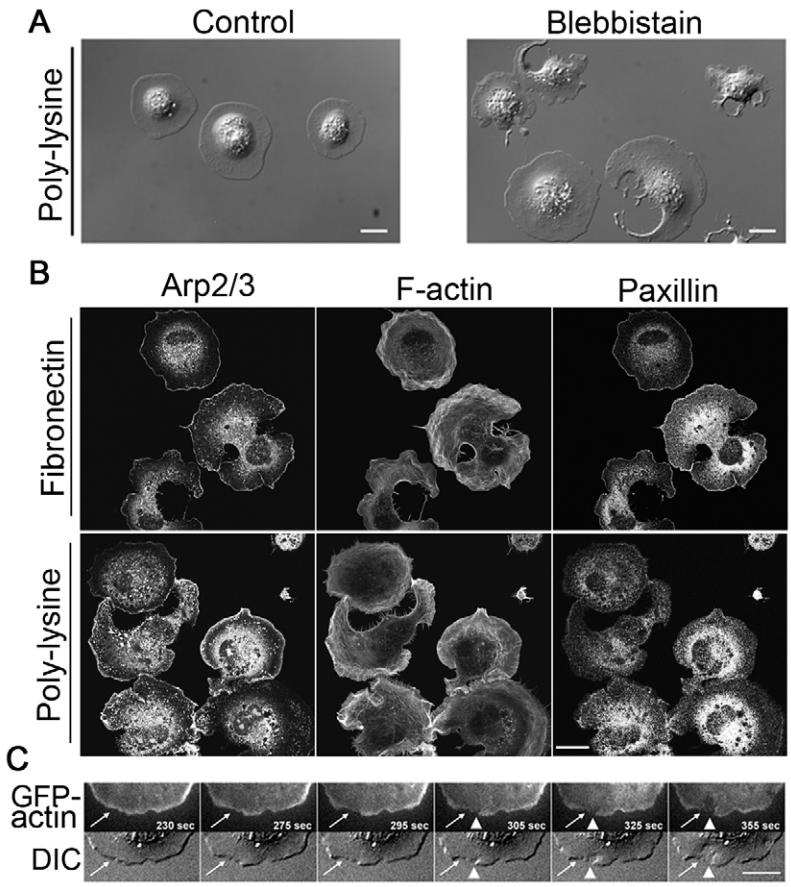


**Fig. 5. Unbalanced actin assembly, not the adhesion of cell to substrates, accounts for cell fragmentation when NMII is inhibited.** (**A**) DIC images of fibroblasts spread on poly-lysine-coated glass for ~20 minutes. Control cells have coherent cytoplasm, whereas blebbistatin-treated cells show loss of cytoplasmic coherence similar to cells spread on fibronectin substrate. (**B**) Staining for Arp2/3, F-actin and paxillin in blebbistatin-treated fibroblasts spread on fibronectin and poly-lysine substrates. The distribution patterns of Arp2/3 and F-actin are similar in NMII-inhibited cells spread on both substrates. There is little or no accumulation of Arp2/3 along the edge of fragmented sites but there is clear accumulation of Arp2/3 along cell edge of other regions of fragmented cells and along the entire cell edge of unfragmented cells. The actin filaments are wavy in NMII-inhibited cells. Much less F-actin is seen at fragmented regions compared to unfragmented regions. Paxillin does not accumulate along the edge of fragmented regions but does along the edge of unfragmented regions when cells spread on fibronectin. By contrast, paxillin is more diffuse in NMII-inhibited cells spreading on poly-lysine. (**C**) Top panels are time-lapse images of TIRF GFP-actin and bottom panels are time-lapse DIC images of a cell spreading on fibronectin substrate. White arrows point to the region where the decrease in GFP-actin intensity precedes the initiation of cytoplasmic fragmentation. Arrowheads show the occurrence of cytoplasmic fragmentation. Scale bars: 20 μm.

or adopt a larger spread area (unfragmented cells) as if under a stretching force from the spreading edges.

There is a concern about a circular aspect of the effect of NMII inhibition on coherence. Because NMII inhibition decreases traction forces, a force-bearing cytoplasmic network is not necessary and one might not form because of the lack of force. However, the CALI experiments show that when NMII is inactivated while within a force-bearing cytoskeletal network, the neighboring active network is able to open a gap in the cytoskeletal network. Thus, we suggest that even a cytoskeletal network under tension requires NMII activity to maintain cytoskeletal coherence. Of note is that cells generate large forces before the formation of stress fibers. Although it can be deduced from previous studies that the actin cytoskeleton might support large forces, it has not, to our knowledge, been directly proven in a background without stress fibers until the study presented here.

A question raised by the cytoplasm fragmentation in NMII-inhibited spreading cells is which occurs first, membrane collapse or disruption of the actomyosin-II network. The relaxation of the actomyosin-II network without plasma membrane collapse in the CALI of MLC experiments supports the idea that compromising the coherence of the actomyosin-II network precedes membrane collapse. This idea is also supported by a previous observation that macro-aperture formation does not induce plasma membrane localization of the lysosomal marker Lamp1, which is associated with membrane wounding (Boyer et al., 2006).

Inhibition of NMII activity causes loss of circumferential actin bundles, stress fibers and integrin-mediated focal adhesions when cells spread on fibronectin. Cells spread on poly-lysine also lack focal adhesions but they do not fragment. Furthermore, inhibition of myosin activity causes fragmentation of cells on poly-lysine. It is still possible that poly-lysine as well as fibronectin-integrin complexes will be altered by changes in the strength of NMII contraction and might play a role in modulating the cytoplasmic coherence. Further investigation in future will be helpful in clarification of this issue.

One might wonder about the possibility of the involvement of stress fibers in the maintenance of cytoplasmic coherence because they are connected with focal adhesions, through which the mechanical forces are transmitted to substrates. We cannot rule out this possibility, but postulate that stress fibers might contribute to the cytoplasmic coherence at a later stage of cell spreading. Our data suggest that the circumferential actin bundles appear to play a primary role in the maintenance of cytoplasmic coherence, at least in early spreading cells, because: (1) circumferential actin bundles develop prior to stress fibers; (2) the initiation of cell fragmentation in spreading cells starts at a time (usually at P1-to-P2 transition and early P2 phase) prior to the formation of stress fibers (usually at late P2 phase); (3) in cells plated on poly-lysine, focal adhesions are not developed (Hotchin and Hall, 1995; Riveline et al., 2001), focal-adhesion-associated stress fibers are very poorly or not developed (Hotchin and Hall, 1995; Kiener et al., 2006), and the prominent actin cytoskeleton structure is more like circumferential actin bundles (Hotchin and Hall, 1995; Kiener et al., 2006); (4) cells spread on poly-lysine substrate do not break (Fig. 5A); and (5) talin-depleted fibroblasts have circumferential actin bundles and no stress fibers and they do not fragment (Zhang et al., 2008).

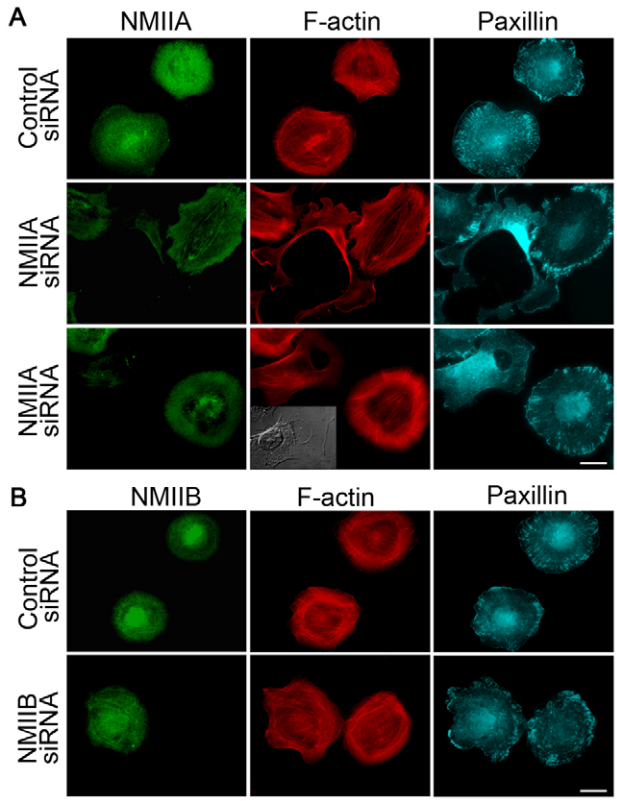


**Fig. 6. Depletion of NMIIA, not NMIIB, causes loss of cytoskeletal coherence.** Cells were transfected with siRNAs for ~96 hours and then spread for ~20-30 minutes on fibronectin-coated coverslips. After fixation, cells were tripled stained for NMIIA or NMIIB, F-actin and paxillin. Colors are pseudo-colors. (**A**) Control siRNA cells have prominent circumferential actin bundles, stress fibers and focal adhesions, which are not present in NMIIA siRNA cells. A large fraction of NMIIA siRNA cells exhibit 'C' shapes, dendritic shapes or have gaps in the actin cytoskeleton. Inset is DIC image of the cell with cytoskeleton gap. (**B**) siRNA NMIIB causes no changes in actin cytoskeleton and focal adhesion. Scale bars: 20 μm.

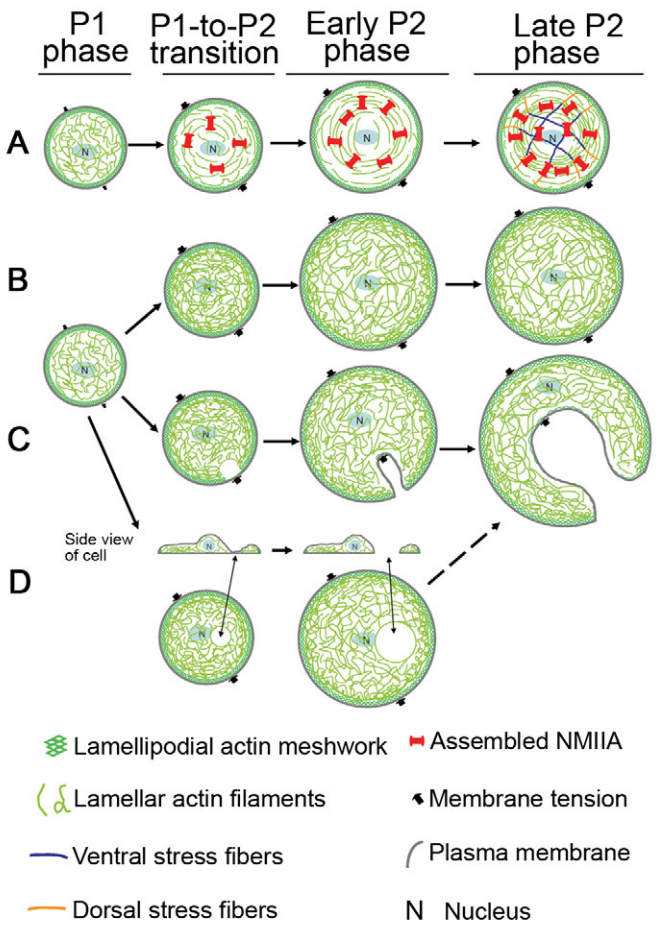


**Fig. 7. Model for development of cytoskeletal coherence and cytoplasmic fragmentation.** The P0 phase of early cell spreading is a basal phase and not covered here. (**A**) There is little NMIIA assembly and contractility and consequent formation of contractile circumferential actin bundles in the fast-spreading P1 phase. As cells approach slow-spreading P2 phase, the assembly and activity of NMIIA increase dramatically. NMIIA contracts and crosslinks actin filaments into a network with tension that prevents cell cytoplasm from being broken by inward plasma membrane tension force. Cells also gain the ability to transmit traction forces from one side of the cell to the other side of the cell. As cell spreading continues through P2 phase, this coherent actin-NMIIA network is expanded. Stress fibers are formed at late P2 stages. (**B**) The coherent actomyosin-II network is not generated without NMIIA activity. Cells are left with a loose actin network that bears all the inward force exerted by membrane tension. Cell-edge regions with normal levels of actin polymerization are able to resist the pressure of the plasma membrane and do not collapse inward. (**C**) When peripheral actin polymerization is decreased even from normal variations in activity, the regions with the lowest level of actin polymerization are the weakest points and are most likely to collapse under membrane tension force. These are the initial membrane fragmentation site(s) during the formation of 'C'- or dendritic-shaped cells. (**D**) If the regions in cell center are depleted of actin filaments due to lack of actin polymerization and/or a high level of actin depolymerization, holes in the center of the actin network develop. The dorsal and ventral plasma membranes then might come close and fuse, leading to the formation of complete holes. These holes might expand under membrane tension force and eventually also result in the formation of 'C' or dendritic shapes.

Microtubules and intermediate filaments are mechanically interconnected with actin cytoskeleton and might have mechanical cellular roles (Ingber, 2003). Published evidence seems to support the notion that the microtubule system might participate in the maintenance of cytoplasmic coherence. For example, simultaneous treatment of cells with nocodazole and the actin-polymerization-promoting reagent PMA occasionally induces the formation of small tail fragments that are separated from the main cell body (Ballestrem et al., 2000). In addition, after stimulation with scatter factor HGF/SF, cells treated with low concentrations of cytochalasin D exhibited cell segregation, which was abolished by addition of nocodazole (Alexandrova et al., 1998). However, treating cells with nocodazole alone in both cases did not induce cell fragmentation, which argues against the idea that microtubules might play a major role in the maintenance of cytoplasmic coherence. Moreover, our data presented here suggest that microtubules are dispensable in cytoplasmic coherence and force transmission; so are intermediate filaments. Still, there is a possibility that microtubules and intermediate filaments play a secondary and modulatory role in actomyosin-dependent maintenance of cytoplasmic coherence. Also, not being involved in the maintenance of cytoplasmic coherence does not rule out their participation in other aspects of cell mechanical stability. For example, we observed oscillation of the nucleus position in spreading cells with disrupted microtubules.

We propose a model (Fig. 7A) for the development of coherence in the actin-NMIIA network that emphasizes several important elements. Rapid assembly of actin filaments occurs at the cell edge and these filaments are rapidly drawn centripetally upon activation of myosin contraction. We suggest that in the fast-spreading P1 phase there is little NMIIA assembly, contractility and subsequent formation of contractile circumferential actin bundles. In P1, the fast cell-edge protrusion is achieved through rapid F-actin assembly that pushes plasma membrane outwards – protrusive force provided by F-actin assembly at plasma membrane is greater than membrane resistance. As the cell approaches the slow-spreading P2 phase, the assembly of NMIIA increases dramatically and NMIIA contraction crosslinks F-actin into a continuous contractile network with force-bearing ability that prevents the cytoskeleton from being broken by forces of membrane tension. The NMIIA clusters are dynamic, undergoing active inward movement (Cai et al., 2006; Even-Ram et al., 2007), which is crucial for forming the coherent network. This network also endows cells with the ability to transmit traction forces from one side of the cell to the other side of the cell. NMIIA contraction of F-actin inward slows down cell spreading because both NMIIA contraction and membrane resistance now work against the outward expansion of the actin network. As cell spreading continues through the P2 phase, this coherent actin-NMIIA network is expanded. Stress fibers are formed at late stages of P2 phase and might contribute to the maintenance of cytoplasmic coherence. Eventually, cells spread to a plateau stage with localized periodic cell-edge protrusions and contractions when the protrusive force is counterbalanced by NMII contraction and plasma membrane tension.

The circumferential actin bundles are formed by end-to-end annealing of short actin bundles through NMII contraction (Hotulainen and Lappalainen, 2006). The lack of NMIIA activity prevents formation of circumferential actin bundles and stress fibers. Thus, the coherent contractile actomyosin network cannot be generated (Fig. 7B). Consequently, only a loosely connected actin network resists the inward forces of the membrane tension (Sheetz et al., 2006). Assuming membrane tension along the cell edge is uniform (Keren et al., 2008), cell edge regions with normal levels of actin polymerization are able to resist the pressure of the plasma membrane and do not collapse inward. When peripheral actin polymerization is decreased, even from normal variations in activity, the regions with the lowest level of actin polymerization are the weakest points and are most likely to collapse under membrane tension. Collapse at one site (Fig. 7B) causes development of 'C' shapes, and collapse at multiple sites results in dendritic-shaped cells. Depletion of actin filaments in the center leads to internal holes that probably result from fusion of dorsal and ventral plasma membrane.

Consistent with this model, our results show that circumferential actin bundles and stress fibers are lost after inhibition of NMII activity, which is in line with two recent studies (Hirata et al., 2009; Senju and Miyata, 2009). The lamellar regions in NMII-inhibited cells are filled with wavy actin filament bundles that belie the loss of tension on the fibers. Initiation of collapse occurs at sites where actin assembly is the lowest. Further, NMII is disorganized and mislocalized. The effects of the small molecule inhibitors on cytoplasmic coherence are reversible, indicating that the processes involved in assembling a coherent cytoskeleton can occur even after cells have spread. In previous studies of actomyosin network dynamics, rapid turnover is found for both myosin and actin filaments, even in fully spread cells (Ponti et al., 2004; Verkhovsky et al., 1995). Actin filament assembly at adhesive contacts is observed and appears to be stimulated by force (Endlich et al., 2007). This is consistent with a dynamic model of the cytoskeleton wherein coherence is established by contraction eliciting additional actin polymerization (O.R. and M.P.S., unpublished observation).

RNA interference (RNAi) depletion of NMII indicates that NMIIA, but not NMIIB, is required for formation of contractile circumferential actin bundles and consequently for cytoplasmic coherence. This is in accord with their differential distributions (Fig. 2A) (Hirata et al., 2009), determined by their C-terminal tails (Ronen and Ravid, 2009; Sandquist and Means, 2008; Vicente-Manzanares et al., 2008), and with their possible different activation states (Hirata et al., 2009) and roles in focal adhesion and stress-fiber formation (Even-Ram et al., 2007; Lo et al., 2004). The fact that ROCK inhibition and depletion of NMIIA generate similar phenotypic changes in cytoplasmic coherence in fibroblasts is consistent with the observation that ROCK preferentially phosphorylates the MLC associated with NMIIA in tumor cells (Sandquist et al., 2006). Although a similar mechanical role of NMIIA is also observed in platelets (Calaminus et al., 2007), the organization of nucleated cell cytoplasm is very different from platelets, and nucleated cells often have multiple myosin isoforms with overlapping functions (Bao et al., 2007; Wylie and Chantler, 2008). Thus, we suggest that the formation of a coherent cytoskeleton in spreading cells involves mechanical condensation of actin filament bundles and NMIIA-dependent movement over long distances in the cytoplasm.

## Materials and Methods

### Antibodies and materials

NMIIA and NMIIC polyclonal antibodies were a gift from Robert Adelstein (National Institutes of Health, Bethesda, MD). NMIIB monoclonal antibody (clone CMII 23) was obtained from Developmental Studies, Hybridoma Bank, University of Iowa. Other materials and their suppliers were as follows: NMIIB polyclonal antibody (Covance); monoclonal GAPDH antibody (Abcam); monoclonal paxillin antibody (Sigma); Arp2/3 antibody (Sigma); TMP-fluorescein (Activemotif); rhodamine-phalloidin, all fluorophore-conjugated secondary antibodies and Calcein-AM (Molecular Probes); blebbistatin and Y27632 (Calbiochem); fibronectin (Roche); and poly-lysine (Sigma). GFP-actin was obtained from Nils C. Gauthier, Columbia University, New York, NY. GFP-caldesmon has been described elsewhere (Helfman et al., 1999).

### Cell culture and plasmid transfection

The mouse embryonic fibroblast cells, RPTP$\alpha^{+/+}$ (Cai et al., 2006), which were primarily used here, NIH3T3 cells and human adrenal carcinoma SW13 cells (from Ronald K. H. Liem, Columbia University, New York, NY) were cultured in Dulbecco's modified Eagle's medium (Invitrogen) supplemented with 10% FBS, 10% NCS, and 5% FBS, respectively. Plasmid transfection was performed with FuGene 6 (Roche).

### DIC and TIRF, and bright-field microscopy of cell spreading

Coverslips were prepared as previously described (Cai et al., 2006). Cells were trypsinized, resuspended in complete culture medium, and then incubated for ~40 minutes at 37°C with or without NMII inhibitors. For TIRF microscopy of cell-spreading, 0.2 μM calcein-AM was added during incubation. Coverslips and pillars were coated with 10 ug/ml of fibronectin or 30 ug/ml of poly-lysine for cell spreading assay.

DIC time-lapse sequential cell images were captured with an Olympus PIanApo 20× oil objective on an Olympus IX81 inverted microscope. TIRF time-lapse sequential images were captured with a 20× water objective on a homemade upright microscope as described elsewhere (Cai et al., 2006). Bright-field images of pillar tips were captured with a LUCPlanFI 40× air objective on an Olympus IX81 inverted microscope. All microscopes were equipped with cooled CCD cameras (Roper Scientific) and temperature control boxes.

### CALI assay

MLC-eDHFR construct was prepared by replacing EGFP in pEGFP-N3-MLC (Tamada et al., 2007) with eDHFR amplified by PCR. The 488 nm Coherent Innova Argon laser beam was split into two by an 80/20 splitter. The weaker beam was used for imaging fluorescein-labeled cells. To minimize photodamage to cells, TIRF, instead of epifluorescence, images were taken to visualize the pre- and post-CALI fluorescence. The stronger beam was used for irradiation and the on-off was controlled

by a shutter. The 'on' time was 1 second in the experiment. The stronger beam was directed and focused to a ~7.0-μm diameter spot using an Olympus PIan Apo 60× 1.45 oil objective on an Olympus IX81 inverted microscope. The irradiation beam power was 3.6 mW at specimen plane.

#### Silencing of NMII

NMII isoform-specific siRNAs and control siRNA were smart pools from Dharmarcon (Chicago, IL). siRNA transfection was conducted using DharmaFECT1 transfection reagent. The day before transfection, cells were plated in 12-well plates. At 72 hours after transfection with 90 nM siRNAs, cells were replated. Then 24 hours later, cells were collected for analyses.

#### Western blot and immunofluorescence

Western blot analysis and immunofluorescence staining were performed as described elsewhere (Cai et al., 2006). Epifluorescence images were taken on an Olympus IX81 inverted microscope (objective, Olympus PIanApo 60× 1.45 NA oil) and confocal images were taken on an Olympus Fluoview FV500 laser scanning confocal microscope with Argon 488 nm, HeNe-G 543 nm and HeNe-R 633 nm beams (objective, Olympus PIanApo 60× 1.45 NA oil).

#### Cell area measurement, force measurement, force mapping and statistical analyses

Cell area measurement was performed using the particle analysis function in ImageJ. Force measurement was performed as described previously (Cai et al., 2006). Force mapping was done using a custom function in Igor. All statistical analyses were performed using a Student's *t*-test tool.

We thank Robert S. Adelstein for NMIIA and NMIIC antibodies. We thank Ronald K. H. Liem for human adrenal carcinoma SW13 cells. We thank Simon Moore, Tomas Perez, Pere Roca-Cusachs, and Armando Del Rio Hernandez for critical reading of this manuscript. We also thank Alexandre Saez and all other Sheetz laboratory members for their support. This work is supported by a NIH grant (5R01GM036277) to M.P.S. The authors have no conflict of interests. Deposited in PMC for release after 12 months.

Supplementary material available online at
http://jcs.biologists.org/cgi/content/full/123/3/413/DC1

## References

**Alexandrova, A. Y., Dugina, V. B., Ivanova, O. Y., Kaverina, I. N. and Vasiliev, J. M.** (1998). Scatter factor induces segregation of multinuclear cells into several discrete motile domains. *Cell Motil. Cytoskeleton* **39**, 147-158.

**Balaban, N. Q., Schwarz, U. S., Riveline, D., Goichberg, P., Tzur, G., Sabanay, I., Mahalu, D., Safran, S., Bershadsky, A., Addadi, L. et al.** (2001). Force and focal adhesion assembly: a close relationship studied using elastic micropatterned substrates. *Nat. Cell Biol.* **3**, 466-472.

**Ballestrem, C., Wehrle-Haller, B., Hinz, B. and Imhof, B. A.** (2000). Actin-dependent lamellipodia formation and microtubule-dependent tail retraction control-directed cell migration. *Mol. Biol. Cell* **11**, 2999-3012.

**Bao, J., Ma, X., Liu, C. and Adelstein, R. S.** (2007). Replacement of nonmuscle myosin II-B with II-A rescues brain but not cardiac defects in mice. *J. Biol. Chem.* **282**, 22102-22111.

**Bar-Ziv, R., Tlusty, T., Moses, E., Safran, S. A. and Bershadsky, A.** (1999). Pearling in cells: a clue to understanding cell shape. *Proc. Natl. Acad. Sci. USA* **96**, 10140-10145.

**Beningo, K. A., Hamao, K., Dembo, M., Wang, Y. L. and Hosoya, H.** (2006). Traction forces of fibroblasts are regulated by the Rho-dependent kinase but not by the myosin light chain kinase. *Arch. Biochem. Biophys.* **456**, 224-231.

**Bertet, C., Sulak, L. and Lecuit, T.** (2004). Myosin-dependent junction remodelling controls planar cell intercalation and axis elongation. *Nature* **429**, 667-671.

**Boyer, L., Doye, A., Rolando, M., Flatau, G., Munro, P., Gounon, P., Clement, R., Pulcini, C., Popoff, M. R., Mettouchi, A. et al.** (2006). Induction of transient macroapertures in endothelial cells through RhoA inhibition by Staphylococcus aureus factors. *J. Cell Biol.* **173**, 809-819.

**Brangwynne, C. P., MacKintosh, F. C., Kumar, S., Geisse, N. A., Talbot, J., Mahadevan, L., Parker, K. K., Ingber, D. E. and Weitz, D. A.** (2006). Microtubules can bear enhanced compressive loads in living cells because of lateral reinforcement. *J. Cell Biol.* **173**, 733-741.

**Burton, K., Park, J. H. and Taylor, D. L.** (1999). Keratocytes generate traction forces in two phases. *Mol. Biol. Cell* **10**, 3745-3769.

**Cai, Y. and Sheetz, M. P.** (2009). Force propagation across cells: mechanical coherence of dynamic cytoskeletons. *Curr. Opin. Cell Biol.* **21**, 47-50.

**Cai, Y., Biais, N., Giannone, G., Tanase, M., Jiang, G., Hofman, J. M., Wiggins, C. H., Silberzan, P., Buguin, A., Ladoux, B. et al.** (2006). Nonmuscle myosin IIA-dependent force inhibits cell spreading and drives F-actin flow. *Biophys. J.* **91**, 3907-3920.

**Calaminus, S. D., Auger, J. M., McCarty, O. J., Wakelam, M. J., Machesky, L. M. and Watson, S. P.** (2007). MyosinIIa contractility is required for maintenance of platelet structure during spreading on collagen and contributes to thrombus stability. *J. Thromb. Haemost.* **5**, 2136-2145.

**Calloway, N. T., Choob, M., Sanz, A., Sheetz, M. P., Miller, L. W. and Cornish, V. W.** (2007). Optimized fluorescent trimethoprim derivatives for in vivo protein labeling. *Chembiochem.* **8**, 767-774.

**Chang, Y. C., Nalbant, P., Birkenfeld, J., Chang, Z. F. and Bokoch, G. M.** (2008). GEF-H1 couples nocodazole-induced microtubule disassembly to cell contractility via RhoA. *Mol. Biol. Cell* **19**, 2147-2153.

**Conti, M. A. and Adelstein, R. S.** (2008). Nonmuscle myosin II moves in new directions. *J. Cell Sci.* **121**, 11-18.

**Cramer, L. P. and Mitchison, T. J.** (1995). Myosin is involved in postmitotic cell spreading. *J. Cell Biol.* **131**, 179-189.

**Danowski, B. A.** (1989). Fibroblast contractility and actin organization are stimulated by microtubule inhibitors. *J. Cell Sci.* **93**, 255-266.

**de Rooij, J., Kerstens, A., Danuser, G., Schwartz, M. A. and Waterman-Storer, C. M.** (2005). Integrin-dependent actomyosin contraction regulates epithelial cell scattering. *J. Cell Biol.* **171**, 153-164.

**Diefenbach, T. J., Latham, V. M., Yimlamai, D., Liu, C. A., Herman, I. M. and Jay, D. G.** (2002). Myosin 1c and myosin IIB serve opposing roles in lamellipodial dynamics of the neuronal growth cone. *J. Cell Biol.* **158**, 1207-1217.

**du Roure, O., Saez, A., Buguin, A., Austin, R. H., Chavrier, P., Silberzan, P. and Ladoux, B.** (2005). Force mapping in epithelial cell migration. *Proc. Natl. Acad. Sci. USA* **102**, 2390-2395.

**Dubin-Thaler, B. J., Hofman, J. M., Cai, Y., Xenias, H., Spielman, I., Shneidman, A. V., David, L. A., Dobereiner, H. G., Wiggins, C. H. and Sheetz, M. P.** (2008). Quantification of cell edge velocities and traction forces reveals distinct motility modules during cell spreading. *PLoS ONE* **3**, e3735.

**Eckes, B., Dogic, D., Colucci-Guyon, E., Wang, N., Maniotis, A., Ingber, D., Merckling, A., Langa, F., Aumailley, M., Delouvee, A. et al.** (1998). Impaired mechanical stability, migration and contractile capacity in vimentin-deficient fibroblasts. *J. Cell Sci.* **111 (Pt 13)**, 1897-1907.

**Endlich, N., Otey, C. A., Kriz, W. and Endlich, K.** (2007). Movement of stress fibers away from focal adhesions identifies focal adhesions as sites of stress fiber assembly in stationary cells. *Cell Motil. Cytoskeleton* **64**, 966-976.

**Even-Ram, S., Doyle, A. D., Conti, M. A., Matsumoto, K., Adelstein, R. S. and Yamada, K. M.** (2007). Myosin IIA regulates cell motility and actomyosin-microtubule crosstalk. *Nat. Cell Biol.* **9**, 299-309.

**Footer, M. J., Kerssemakers, J. W., Theriot, J. A. and Dogterom, M.** (2007). Direct measurement of force generation by actin filament polymerization using an optical trap. *Proc. Natl. Acad. Sci. USA* **104**, 2181-2186.

**Galbraith, C. G. and Sheetz, M. P.** (1999). Keratocytes pull with similar forces on their dorsal and ventral surfaces. *J. Cell Biol.* **147**, 1313-1324.

**Giannone, G., Dubin-Thaler, B. J., Dobereiner, H. G., Kieffer, N., Bresnick, A. R. and Sheetz, M. P.** (2004). Periodic lamellipodial contractions correlate with rearward actin waves. *Cell* **116**, 431-443.

**Goldman, R. D., Grin, B., Mendez, M. G. and Kuczmarski, E. R.** (2008). Intermediate filaments: versatile building blocks of cell structure. *Curr. Opin. Cell Biol.* **20**, 28-34.

**Grosheva, I., Vittitow, J. L., Goichberg, P., Gabelt, B. T., Kaufman, P. L., Borras, T., Geiger, B. and Bershadsky, A. D.** (2006). Caldesmon effects on the actin cytoskeleton and cell adhesion in cultured HTM cells. *Exp. Eye Res.* **82**, 945-958.

**Helfman, D. M., Levy, E. T., Berthier, C., Shtutman, M., Riveline, D., Grosheva, I., Lachish-Zalait, A., Elbaum, M. and Bershadsky, A. D.** (1999). Caldesmon inhibits nonmuscle cell contractility and interferes with the formation of focal adhesions. *Mol. Biol. Cell* **10**, 3097-3112.

**Hirata, N., Takahashi, M. and Yazawa, M.** (2009). Diphosphorylation of regulatory light chain of myosin IIA is responsible for proper cell spreading. *Biochem. Biophys. Res. Commun.* **381**, 682-687.

**Holwell, T. A., Schweitzer, S. C. and Evans, R. M.** (1997). Tetracycline regulated expression of vimentin in fibroblasts derived from vimentin null mice. *J. Cell Sci.* **110 (Pt 16)**, 1947-1956.

**Hotchin, N. A. and Hall, A.** (1995). The assembly of integrin adhesion complexes requires both extracellular matrix and intracellular rho/rac GTPases. *J. Cell Biol.* **131**, 1857-1865.

**Hotulainen, P. and Lappalainen, P.** (2006). Stress fibers are generated by two distinct actin assembly mechanisms in motile cells. *J. Cell Biol.* **173**, 383-394.

**Ingber, D. E.** (2003). Tensegrity I. Cell structure and hierarchical systems biology. *J. Cell Sci.* **116**, 1157-1173.

**Ivanov, A. I., Bachar, M., Babbin, B. A., Adelstein, R. S., Nusrat, A. and Parkos, C. A.** (2007). A Unique role for nonmuscle myosin heavy chain IIA in regulation of epithelial apical junctions. *PLoS ONE* **2**, e658.

**Keren, K., Pincus, Z., Allen, G. M., Barnhart, E. L., Marriott, G., Mogilner, A. and Theriot, J. A.** (2008). Mechanism of shape determination in motile cells. *Nature* **453**, 475-480.

**Kiener, H. P., Lee, D. M., Agarwal, S. K. and Brenner, M. B.** (2006). Cadherin-11 induces rheumatoid arthritis fibroblast-like synoviocytes to form lining layers in vitro. *Am. J. Pathol.* **168**, 1486-1499.

**Lemmon, C. A., Chen, C. S. and Romer, L. H.** (2009). Cell traction forces direct fibronectin matrix assembly. *Biophys. J.* **96**, 729-738.

**Lo, C. M., Buxton, D. B., Chua, G. C., Dembo, M., Adelstein, R. S. and Wang, Y. L.** (2004). Nonmuscle myosin IIb is involved in the guidance of fibroblast migration. *Mol. Biol. Cell* **15**, 982-989.

**Marston, S., Burton, D., Copeland, O., Fraser, I., Gao, Y., Hodgkinson, J., Huber, P., Levine, B., el-Mezgueldi, M. and Notarianni, G.** (1998). Structural interactions between actin, tropomyosin, caldesmon and calcium binding protein and the regulation of smooth muscle thin filaments. *Acta. Physiol. Scand.* **164**, 401-414.

**Martin, A. C., Kaschube, M. and Wieschaus, E. F.** (2009). Pulsed contractions of an actin-myosin network drive apical constriction. *Nature* **457**, 495-499.
**Miller, L. W., Cai, Y., Sheetz, M. P. and Cornish, V. W.** (2005). In vivo protein labeling with trimethoprim conjugates: a flexible chemical tag. *Nat. Methods* **2**, 255-257.
**Pelham, R. J., Jr and Wang, Y.** (1999). High resolution detection of mechanical forces exerted by locomoting fibroblasts on the substrate. *Mol. Biol. Cell* **10**, 935-945.
**Pollard, T. D. and Borisy, G. G.** (2003). Cellular motility driven by assembly and disassembly of actin filaments. *Cell* **112**, 453-465.
**Polte, T. R., Eichler, G. S., Wang, N. and Ingber, D. E.** (2004). Extracellular matrix controls myosin light chain phosphorylation and cell contractility through modulation of cell shape and cytoskeletal prestress. *Am. J. Physiol. Cell Physiol.* **286**, C518-C528.
**Ponti, A., Machacek, M., Gupton, S. L., Waterman-Storer, C. M. and Danuser, G.** (2004). Two distinct actin networks drive the protrusion of migrating cells. *Science* **305**, 1782-1786.
**Prass, M., Jacobson, K., Mogilner, A. and Radmacher, M.** (2006). Direct measurement of the lamellipodial protrusive force in a migrating cell. *J. Cell Biol.* **174**, 767-772.
**Raucher, D. and Sheetz, M. P.** (2000). Cell spreading and lamellipodial extension rate is regulated by membrane tension. *J. Cell Biol.* **148**, 127-136.
**Riveline, D., Zamir, E., Balaban, N. Q., Schwarz, U. S., Ishizaki, T., Narumiya, S., Kam, Z., Geiger, B. and Bershadsky, A. D.** (2001). Focal contacts as mechanosensors: externally applied local mechanical force induces growth of focal contacts by an mDia1-dependent and ROCK-independent mechanism. *J. Cell Biol.* **153**, 1175-1186.
**Ronen, D. and Ravid, S.** (2009). Myosin II tailpiece determines its paracrystal structure, filament assembly properties, and cellular localization. *J. Biol. Chem.* **284**, 24948-24957.
**Sandquist, J. C. and Means, A. R.** (2008). The C-terminal tail region of nonmuscle myosin II directs isoform-specific distribution in migrating cells. *Mol. Biol. Cell* **19**, 5156-5167.
**Sandquist, J. C., Swenson, K. I., Demali, K. A., Burridge, K. and Means, A. R.** (2006). Rho kinase differentially regulates phosphorylation of nonmuscle myosin II isoforms A and B during cell rounding and migration. *J. Biol. Chem.* **281**, 35873-35883.
**Sarria, A. J., Nordeen, S. K. and Evans, R. M.** (1990). Regulated expression of vimentin cDNA in cells in the presence and absence of a preexisting vimentin filament network. *J. Cell Biol.* **111**, 553-565.
**Schaub, S., Bohnet, S., Laurent, V. M., Meister, J. J. and Verkhovsky, A. B.** (2007). Comparative maps of motion and assembly of filamentous actin and myosin II in migrating cells. *Mol. Biol. Cell* **18**, 3723-3732.
**Schliwa, M.** (1982). Action of cytochalasin D on cytoskeletal networks. *J. Cell Biol.* **92**, 79-91.
**Senju, Y. and Miyata, H.** (2009). The role of actomyosin contractility in the formation and dynamics of actin bundles during fibroblast spreading. *J. Biochem.* **145**, 137-150.
**Sheetz, M. P.** (2001). Cell control by membrane-cytoskeleton adhesion. *Nat. Rev. Mol. Cell. Biol.* **2**, 392-396.
**Sheetz, M. P., Sable, J. E. and Dobereiner, H. G.** (2006). Continuous membrane-cytoskeleton adhesion requires continuous accommodation to lipid and cytoskeleton dynamics. *Annu. Rev. Biophys. Biomol. Struct.* **35**, 417-434.
**Shewan, A. M., Maddugoda, M., Kraemer, A., Stehbens, S. J., Verma, S., Kovacs, E. M. and Yap, A. S.** (2005). Myosin 2 is a key Rho kinase target necessary for the local concentration of E-cadherin at cell-cell contacts. *Mol. Biol. Cell* **16**, 4531-4542.
**Sims, J. R., Karp, S. and Ingber, D. E.** (1992). Altering the cellular mechanical force balance results in integrated changes in cell, cytoskeletal and nuclear shape. *J. Cell Sci.* **103 (Pt 4)**, 1215-1222.
**Small, J. V. and Resch, G. P.** (2005). The comings and goings of actin: coupling protrusion and retraction in cell motility. *Curr. Opin. Cell Biol.* **17**, 517-523.
**Sunyer, R., Trepat, X., Fredberg, J. J., Farre, R. and Navajas, D.** (2009). The temperature dependence of cell mechanics measured by atomic force microscopy. *Phys. Biol.* **6**, 25009.
**Tamada, M., Perez, T. D., Nelson, W. J. and Sheetz, M. P.** (2007). Two distinct modes of myosin assembly and dynamics during epithelial wound closure. *J. Cell Biol.* **176**, 27-33.
**Tan, J. L., Tien, J., Pirone, D. M., Gray, D. S., Bhadriraju, K. and Chen, C. S.** (2003). Cells lying on a bed of microneedles: an approach to isolate mechanical force. *Proc. Natl. Acad. Sci. USA* **100**, 1484-1489.
**Totsukawa, G., Wu, Y., Sasaki, Y., Hartshorne, D. J., Yamakita, Y., Yamashiro, S. and Matsumura, F.** (2004). Distinct roles of MLCK and ROCK in the regulation of membrane protrusions and focal adhesion dynamics during cell migration of fibroblasts. *J. Cell Biol.* **164**, 427-439.
**Undyala, V. V., Dembo, M., Cembrola, K., Perrin, B. J., Huttenlocher, A., Elce, J. S., Greer, P. A., Wang, Y. L. and Beningo, K. A.** (2008). The calpain small subunit regulates cell-substrate mechanical interactions during fibroblast migration. *J. Cell Sci.* **121**, 3581-3588.
**Verkhovsky, A. B., Svitkina, T. M. and Borisy, G. G.** (1995). Myosin II filament assemblies in the active lamella of fibroblasts: their morphogenesis and role in the formation of actin filament bundles. *J. Cell Biol.* **131**, 989-1002.
**Verkhovsky, A. B., Svitkina, T. M. and Borisy, G. G.** (1999). Self-polarization and directional motility of cytoplasm. *Curr. Biol.* **9**, 11-20.
**Vicente-Manzanares, M., Koach, M. A., Whitmore, L., Lamers, M. L. and Horwitz, A. F.** (2008). Segregation and activation of myosin IIB creates a rear in migrating cells. *J. Cell Biol.* **183**, 543-554.
**Vicente-Manzanares, M., Ma, X., Adelstein, R. S. and Horwitz, A. R.** (2009). Non-muscle myosin II takes centre stage in cell adhesion and migration. *Nat. Rev. Mol. Cell. Biol.* **10**, 778-790.
**Wakatsuki, T., Wysolmerski, R. B. and Elson, E. L.** (2003). Mechanics of cell spreading: role of myosin II. *J. Cell Sci.* **116**, 1617-1625.
**Wang, F. S., Liu, C. W., Diefenbach, T. J. and Jay, D. G.** (2003). Modeling the role of myosin 1c in neuronal growth cone turning. *Biophys. J.* **85**, 3319-3328.
**Waterman-Storer, C. M. and Salmon, E.** (1999). Positive feedback interactions between microtubule and actin dynamics during cell motility. *Curr. Opin. Cell Biol.* **11**, 61-67.
**Wylie, S. R. and Chantler, P. D.** (2008). Myosin IIC: a third molecular motor driving neuronal dynamics. *Mol. Biol. Cell* **19**, 3956-3968.
**Zhang, X., Jiang, G., Cai, Y., Monkley, S. J., Critchley, D. R. and Sheetz, M. P.** (2008). Talin depletion reveals independence of initial cell spreading from integrin activation and traction. *Nat. Cell Biol.* **10**, 1062-1068.
**Zimerman, B., Volberg, T. and Geiger, B.** (2004). Early molecular events in the assembly of the focal adhesion-stress fiber complex during fibroblast spreading. *Cell Motil Cytoskeleton* **58**, 143-159.

Journal of Cell Science